CHAPTER 4

GEOCHEMISTRY

4.1 Sample Preparation

The carefully selected thirty-five Mae Tha basaltic samples (as previously mentioned in Chapter 3) were prepared for whole-rock chemical analysis by firstly splitting into conveniently-sized fragments and then crushing into small thin chips (approximately 0.5 cm across), using a Rocklabs hydraulic splitter/crusher. These crushed fragments were cautiously chosen to avoid vesicles, amygdale minerals, veinlets, megacrysts and weathered surfaces. The selected chips were blown by compressed air to remove dusty materials. Approximately 50-80 g. aliquots of the clean selected chips were pulverized for a few minutes using a Rocklabs tungsten-carbide ring mill. All the preparation procedures were done in the Department of Geological Sciences, Chiang Mai University.

4.2 Analytical Techniques

All the powdered samples were analyzed for 12 major and minor oxides, including SiO_2, TiO_2, Al_2O_3, Fe_2O_3, FeO, MnO, MgO, CaO, Na_2O, K_2O, P_2O_5 and loss on ignition. In addition, these powdered samples were analyzed for Ba, Rb, Sr, Y, Zr, V, Ni and Cr. Four representatives of these samples were analyzed for Nb, Th, U and rare-earth elements such as Ce, La, Nd, Sm, Eu, Tb, Yb and Lu.

Almost all the analyses for major and minor oxides (SiO_2, TiO_2, Al_2O_3, total iron as Fe_2O_3, MnO, MgO, CaO, Na_2O, K_2O, and P_2O_5) were determined using an automated Siemens SRS 3000 Sequential X-ray Spectrometer (wavelength dispersive system) installed at Material Testing Laboratory Section, Electricity Generating Authority of Thailand, Changwat Lampang. These oxides were measured from fusion

discs prepared by mixing 1.5 g sample powder with 7.5 g di-lithiumtetraborate flux. The standard used in these analyses were the international USGS standards: RGM-1, W-2 and BIR-1. Trace elements (Ba, Rb, Sr, Y, Zr, V, Ni and Cr) were analyzed using an automated Philips PW 1400 XRF Spectrometer (wavelength dispersive system) by the staff of Rock and Mineral Analysis Section, Department of Mineral Resources, Bangkok. The fusion discs used in trace-element analysis were prepared with 1 g powdered sample and 5.405 g spectroflux 105. Detection limits for trace element analyses are 10 ppm.

FeO and ignition loss were measured in the Department of Geological Sciences, Chiang Mai University. FeO determination was done by using visual titration, following the modified cold acid decomposition method of Wilson (1955), whereas loss on ignition was gravimetrically determined by heating approximately of 0.5 g of powdered sample at 1,050 °C for 1 hour.

The analyses of Nb, and Th, U and rare-earth elements (herein REE) were performed using X-ray fluorescence and neutron activation techniques, respectively, by the staff of Chemex Labs Ltd. (Canada). The code for Nb analysis is 191 (detection limit 2 ppm), while that for Th, U and rare-earth elements is RE-10 (NAA) of which the detection limits for Th, U, Ce, La, Nd, Sm, Eu, Tb, Yb and Lu are 0.5, 1, 2, 1, 5, 0.1, 0.5, 0.5, 0.5 and 0.1 ppm in respect manner.

4.3 Magmatic Affinities and Rock Types

The studied Mae Tha basaltic rocks (Appendix D) are compositionally basic, as evidenced by their low values for SiO_2 and Mg/(Mg+Fe) (herein mg#) that are in ranges of 46.12-51.23 wt% (average 48.58±1.68 wt%) and 0.60-0.70 (0.65 on average), respectively. It is worth noting here that mg# was calculated assuming an Fe_2O_3/FeO ratio of 0.20 (e.g. Le Roex *et al.*, 1990; Adam, 1990) to minimize the effect of subsolidus oxidation. These basic rocks have variable Na_2O+K_2O contents (5.89-8.10 wt%, 6.80±0.43 on average) with an averaged K_2O/Na_2O ratios of 0.82

±0.20 (0.30-1.19). Their Ni and Cr contents vary from 90 to 251 ppm and from 128 to 329 ppm, respectively. They form a compositional field straddling the demarcation line separating highly alkalic field from mildly alkalic field on total alkalis-silica diagram (Fig. 31). The Nb/Y ratios (1.39-1.75) of representative samples also lie well within the limit of alkalic rocks (Pearce and Cann, 1973; Floyd and Winchester, 1975; Winchester and Floyd, 1977; Pearce, 1982). These imply that they are undoubtedly alkalic rocks that are transitional from trachybasaltic to basanitic series.

According to the discrimination diagram for different rock types of Le Bas *et al.* (1986), these alkalic basaltic lavas are constituted largely by basanite, basaltic trachyandesite and trachybasalt; very few are phonotephrite (Fig. 31). The relative amounts of Na_2O and K_2O for trachybasalts and basaltic trachybasalts signify that they are almost all potassic types, i.e. trachybasalts and shoshonites (Le Bas *et al.*, 1986), respectively. In terms of normative compositions (Appendix D), the presented lavas contain normative nepheline varying from 0.53 to 13.56%.

4.4 Major and Minor Oxides

It is well established that any suite of magmatic rocks related by crystal fractionation and unmodified by extensive crustal contamination should define coherent linear trends on appropriate variation diagrams. In this account, the data for major and minor oxides are plotted against MgO as a parameter for fractionation (Figs. 32 and 33). The data points for SiO_2 and Al_2O_3 form well-defined negative coherent trends on the MgO variation diagram. It is of particular interest that the trend for Al_2O_3 appears to have an inflection point at a MgO content of more or less 6.00 wt%. The existence of an inflection point is well supported by the data of Yamamoto (1991). TiO_2, total iron as FeO (herein FeO*), MnO and CaO bear broad positive correlations with MgO, while Na_2O+K_2O and P_2O_5 increase with advancing fractionation. All the major- and minor- oxide variations suggest that the Mae Tha basaltic rocks are comagmatic. The depletion of FeO*, MnO, CaO and MgO in the

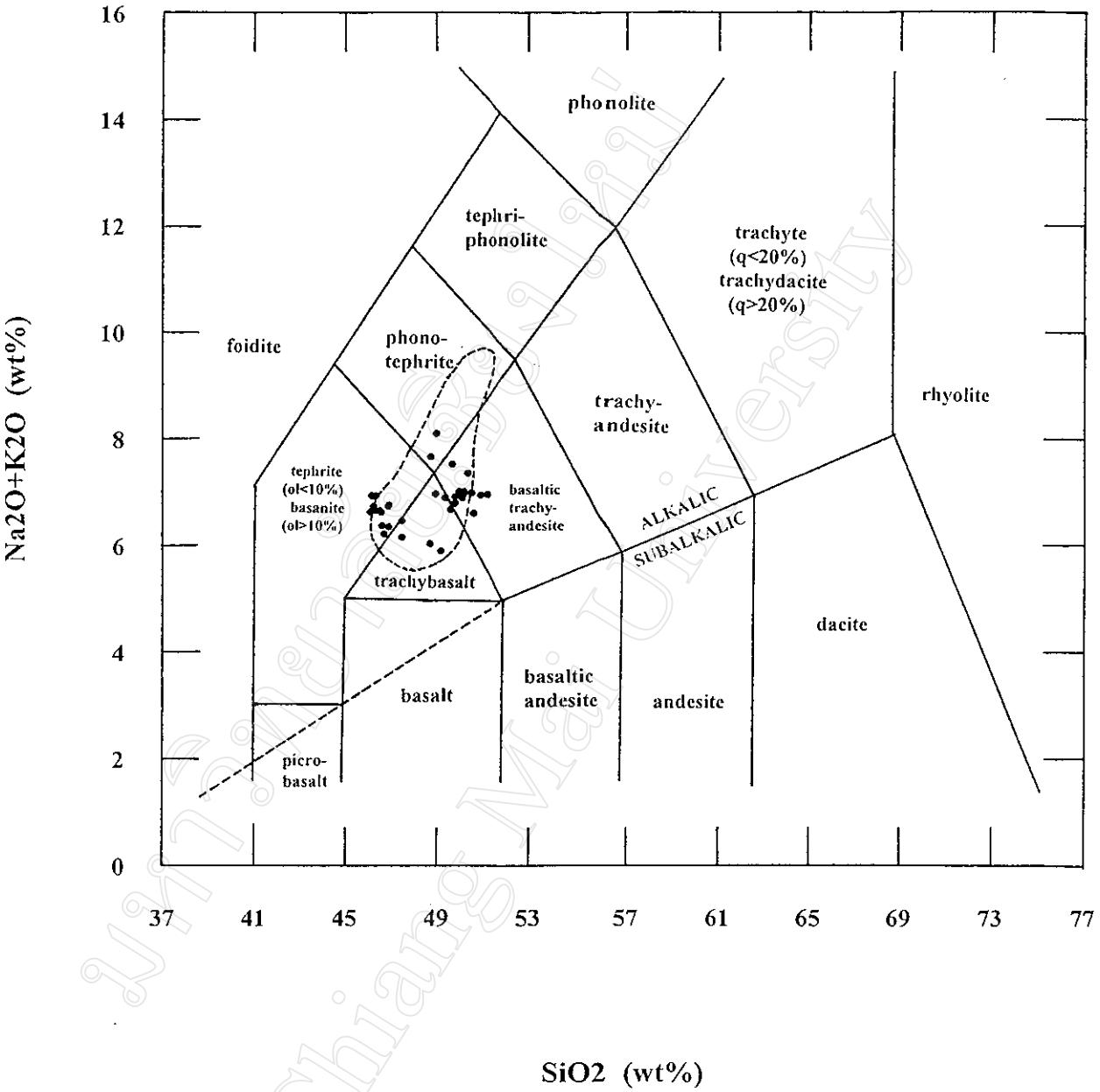

Figure 31 Alkali versus silica plot for the analyzed Mae Tha basalts. Delimited fields for different rock types are after Le Bas *et al.* (1986). Also shown are an alkalic/subalkalic dividing line of Miyashiro (1978), and a compositional field for the Mae Tha basalts of Yamamoto (1991) that is bordered by broken line.

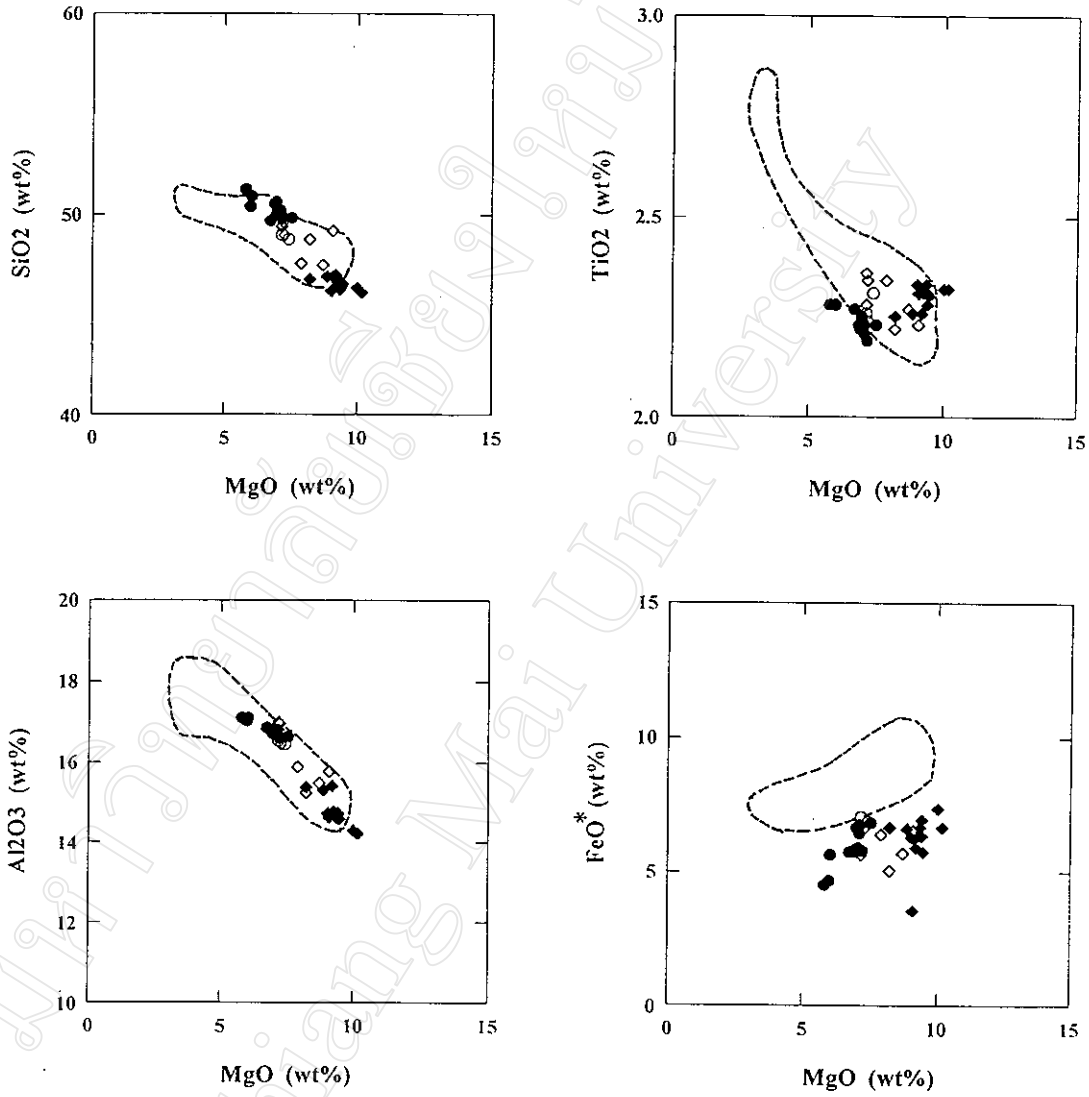

Figure 32 MgO variation diagrams for SiO_2, TiO_2, Al_2O_3 and FeO* in the Mae Tha alkalic basalts (solid circle, basaltic trachyandesite; open circle, phonotephrite; solid diamond, basanite; and open diamond, trachybasalt). The compositional fields of the Mae Tha basalts of Yamamoto (1991), bordered by broken lines, are also shown for comparison.

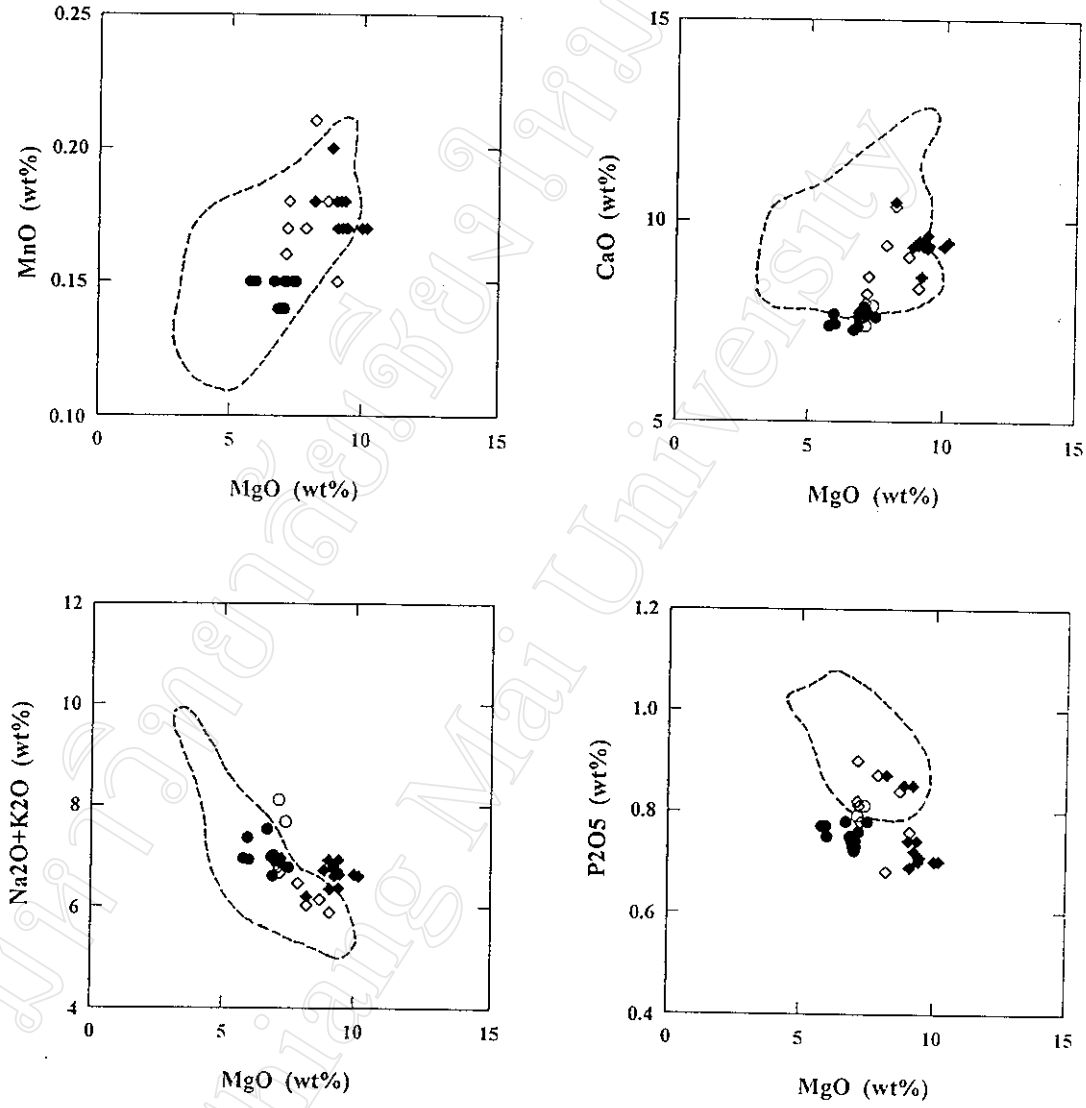

Figure 33 MgO variation diagrams for MnO, CaO, $Na_2O + K_2O$ and P_2O_5 in the Mae Tha alkalic basalts (solid circle, basaltic trachyandesite; open circle, phonotephrite; solid diamond, basanite; and open diamond, trachybasalt). The compositional fields of the Mae Tha basalts of Yamamoto (1991), bordered by broken lines, are also shown for comparison.

more primitive stage signify that the trends are controlled significantly by suppression of Fe-Ti oxide minerals, clinopyroxene and olivine. The slight Al_2O_3 depletion in the more fractionated rocks is possibly due to the onset of plagioclase fractionation. The presence of olivine, clinopyroxene, plagioclase and Fe-Ti oxide phenocrysts/microphenocrysts, as previously discussed in Section 3.2, is consistent with such an interpretation. The inconsistency of TiO_2 pattern in this study and that of Yamamoto may be attributable to the ambiguous TiO_2 data of Yamamoto as evidenced by the incompatibility of TiO_2 and FeO*.

4.5 Trace Elements

Using the same fractionation index as major- and minor-oxide variation diagrams, the abundances of Ba, Rb, Sr, Y and Zr are highly variable at similar values for MgO (Figs. 34 and 35). These may be attributable to the limited MgO values for the studied basalt samples. Ni, Cr and V, however, form well-defined positive trends, signifying that they are compatible elements. The depletion of V and Ni in the more evolved samples corresponds with Fe-Ti oxide and olivine fractionation in respect manner, as previously discussed in Section 4.4. The decrease in Cr with advancing fractionation records the removal of chromian spinel, as expected from the presence of chromian spinel microphenocrysts in the studied samples (see Section 3.2). On grounds of major- and minor-oxide, and trace element variations, the sequence of crystallization for the Mae Tha basalt can be inferred at this stage as follows: olivine + chromian spinel + clinopyroxene + Fe-Ti oxides in the earlier stage and then plagioclase in the late stage.

In basaltic rocks, Ti, Mn, P, Ba, Rb, Sr, Nb, Y, Zr and V are generally regarded as incompatible elements. Nevertheless, the previously discussed geochemical patterns for the Mae Tha basalt, in terms of major and minor oxides, and trace elements, reveal that Ti, Mn and V are compatible elements. Therefore, the actual incompatible elements in the studied basalts include P, Ba, Rb, Sr, Nb, Y and Zr. As the ratios for these incompatible-element pairs are in narrow ranges, e.g. Zr/Nb

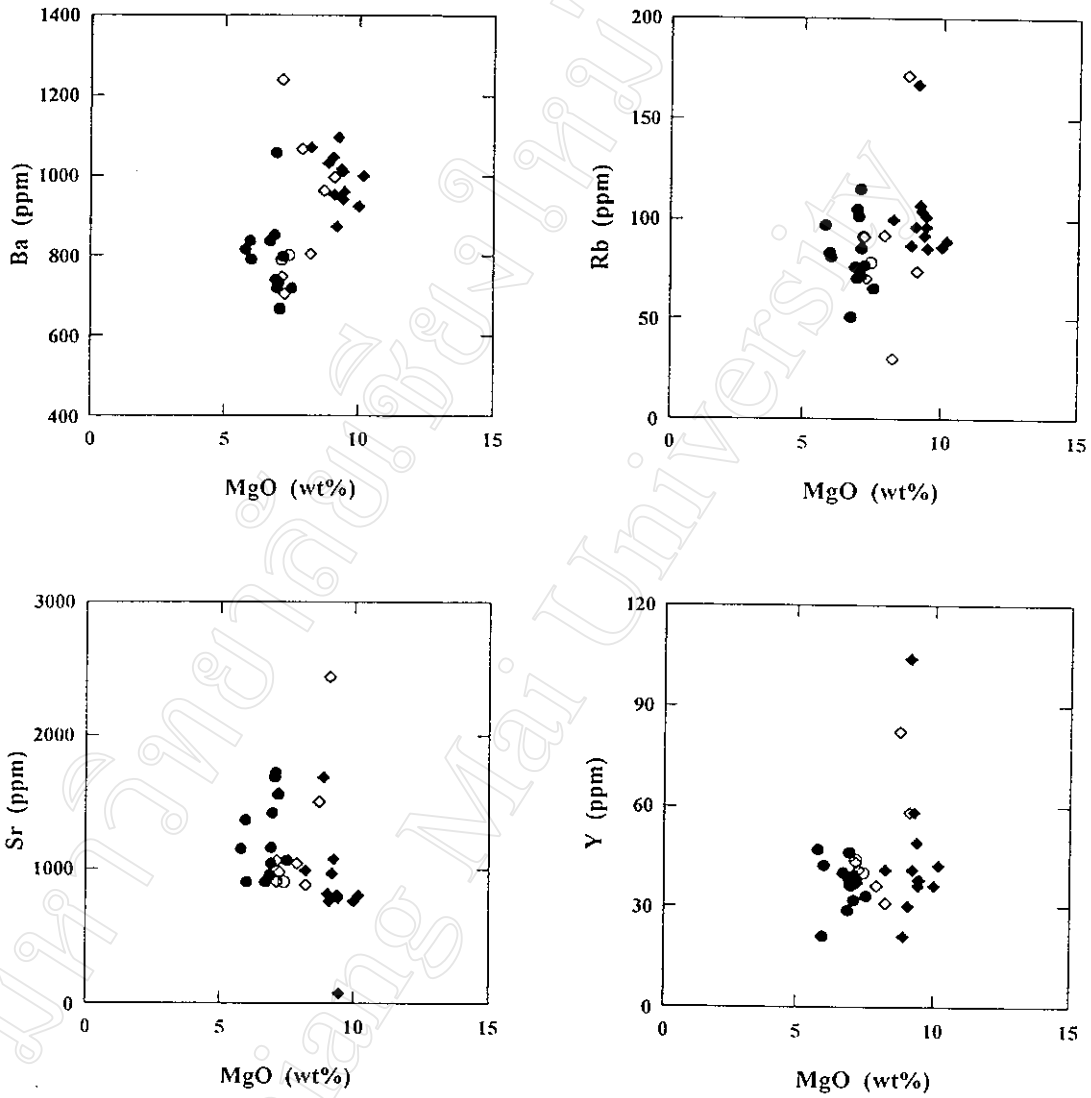

Figure 34 MgO variation diagrams for Ba, Rb, Sr and Y in the Mae Tha alkalic basalts (solid circle, basaltic trachyandesite; open circle, phonotephrite; solid diamond, basanite; and open diamond, trachybasalt).

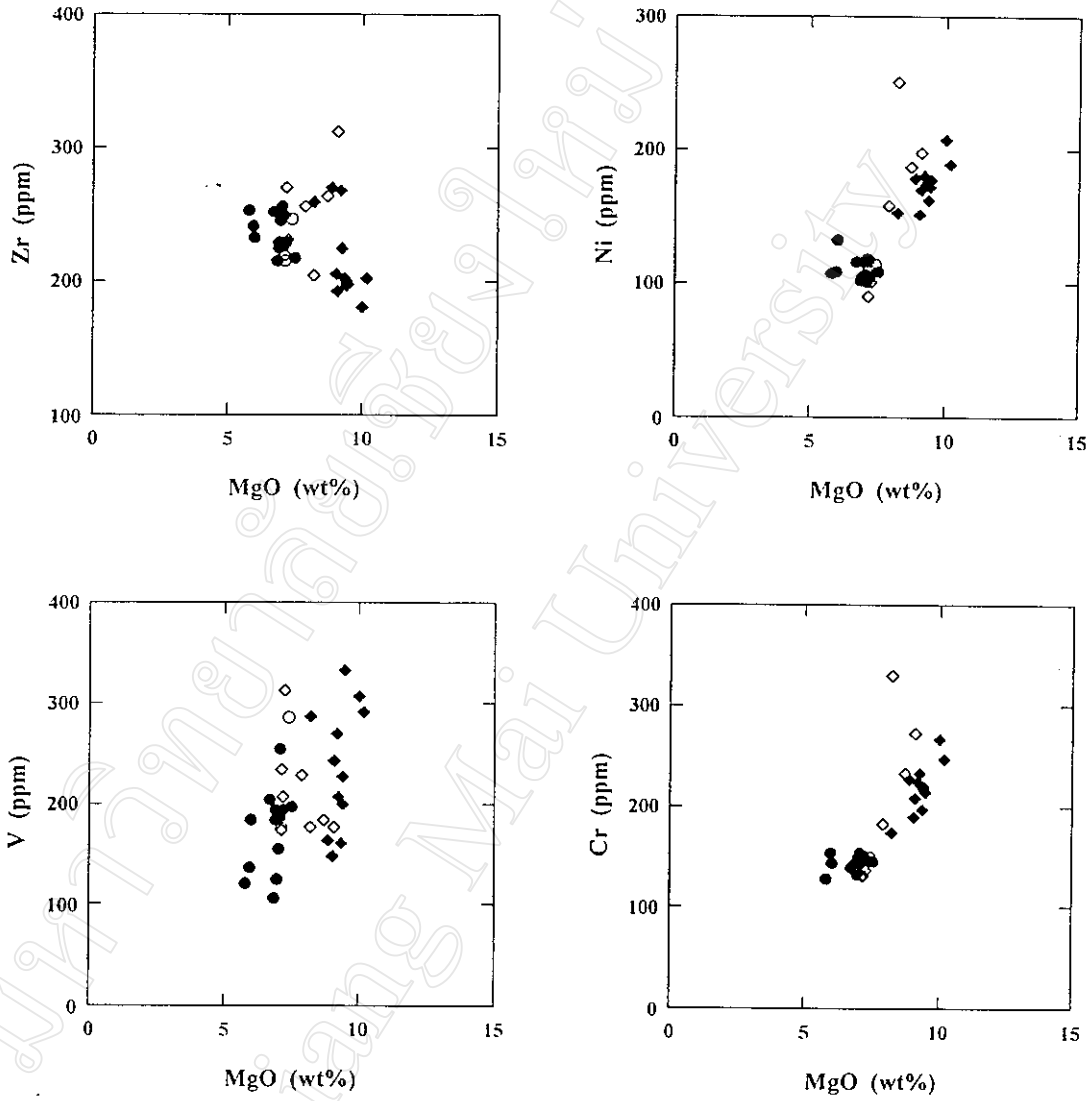

Figure 35 MgO variation diagrams for Zr, Ni, V and Cr in the Mae Tha alkalic basalts (solid circle, basaltic trachyandesite; open circle, phonotephrite; solid diamond, basanite; and open diamond, trachybasalt).

= 3.47 ± 0.10, Nb/Y = 1.55 ± 0.17, Ba/K = 0.04 ± 0.01, P/K = 0.14 ± 0.03, Zr/Ba = 0.26 ± 0.05, Zr/K = 0.011 ± 0.003, Zr/P = 0.07 ± 0.01, Ba/Sr = 1.097 ± 0.04, Ba/P = 0.27 ± 0.05, and Y/Zr = 0.18 ± 0.08 (Appendix E), all the studied basalt samples are interpreted to have a comagmatic origin, as expected from the geochemical patterns discussed above.

Up to present, many empirical diagrams for discriminating tectonic settings of eruption have appeared in literature (e.g. Pearce and Cann, 1973; Pearce and Norry, 1979; Pearce, 1980,1982; Shervais, 1982; Meschede, 1986). These diagrams are largely designed for basalts of tholeiitic affinities; a few can be applied to alkalic basalt and transitional tholeiite. Therefore, the basalts of Mae Tha suite are plotted only in terms of Ti-V (Fig. 36), Ti/Y-Nb/Y (Fig. 36) and Nb-Zr-Y (Fig. 37) to avoid ambiguous results. It appears that the Mae Tha basalts obviously fall in the compositional fields of within-plate alkalic and tholeiitic basalts in the Ti-V and Nb-Zr-Y plots, respectively. However, in the Ti/Y-Nb/Y diagram, their data are immediately close to the fields of both within-plate and mid-ocean ridge basalts.

4.6 Multi-element Patterns

REE analyses for four representatives of the Mae Tha basaltic suite (sample nos. MT 1/A, MT 22, MT 27, and MT 30F1) are reported in Appendix E, and their chondrite-normalized values are plotted in Figure 38. The REE patterns show light rare-earth-element (herein LREE) enrichment with chondrite-normalized La/Sm (herein $(La/Sm)_n$) varying from 3.14 to 3.37 and are relatively depleted in heavy rare-earth elements (herein HREE) with chondrite-normalized Sm/Yb (herein $(Sm/Yb)_n$) ranging from 3.63 to 3.82. These REE patterns are very similar to those of world-wide alkalic basalts. The non-parallel and crosscut patterns may be arisen from analytical errors and/or variable degrees of crustal contamination as illustrated by petrographic evidences. Further isotopic studies are required to assess the hypothesis of crustal contamination.

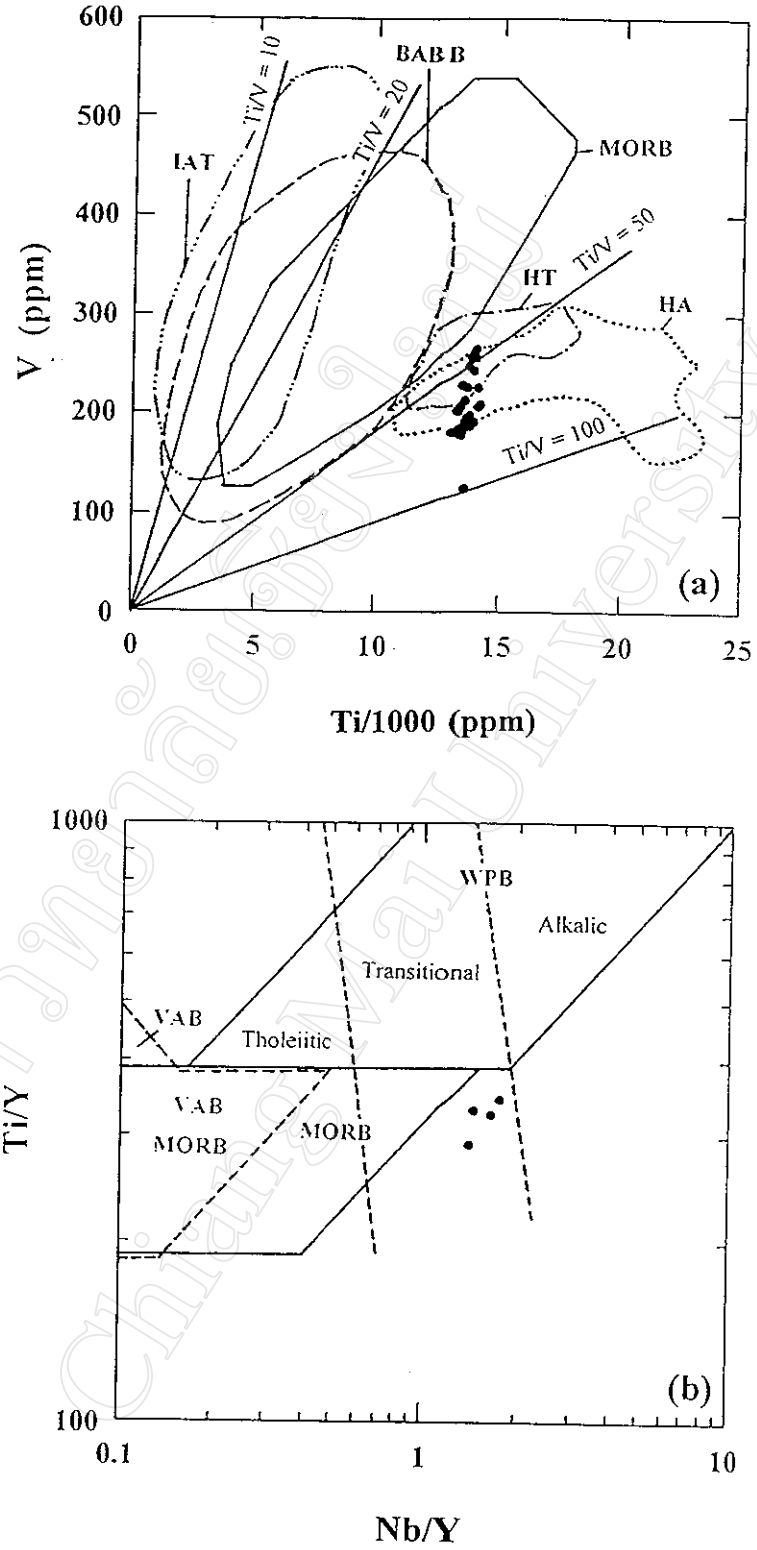

Figure 36 Tectonic discrimination diagrams in terms of (a) Ti and V (after Shervais, 1982), and (b) Ti/Y and Nb/Y (after Pearce, 1982) for the Mae Tha basalts. HA = Hawaiian alkalic basalt, HT = Hawaiian tholeiite, MORB = mid-ocean ridge basalt, BABB = backarc basin basalt, IAT = island-arc tholeiite, WPB = within-plate basalt, and VAB = volcanic arc basalt.

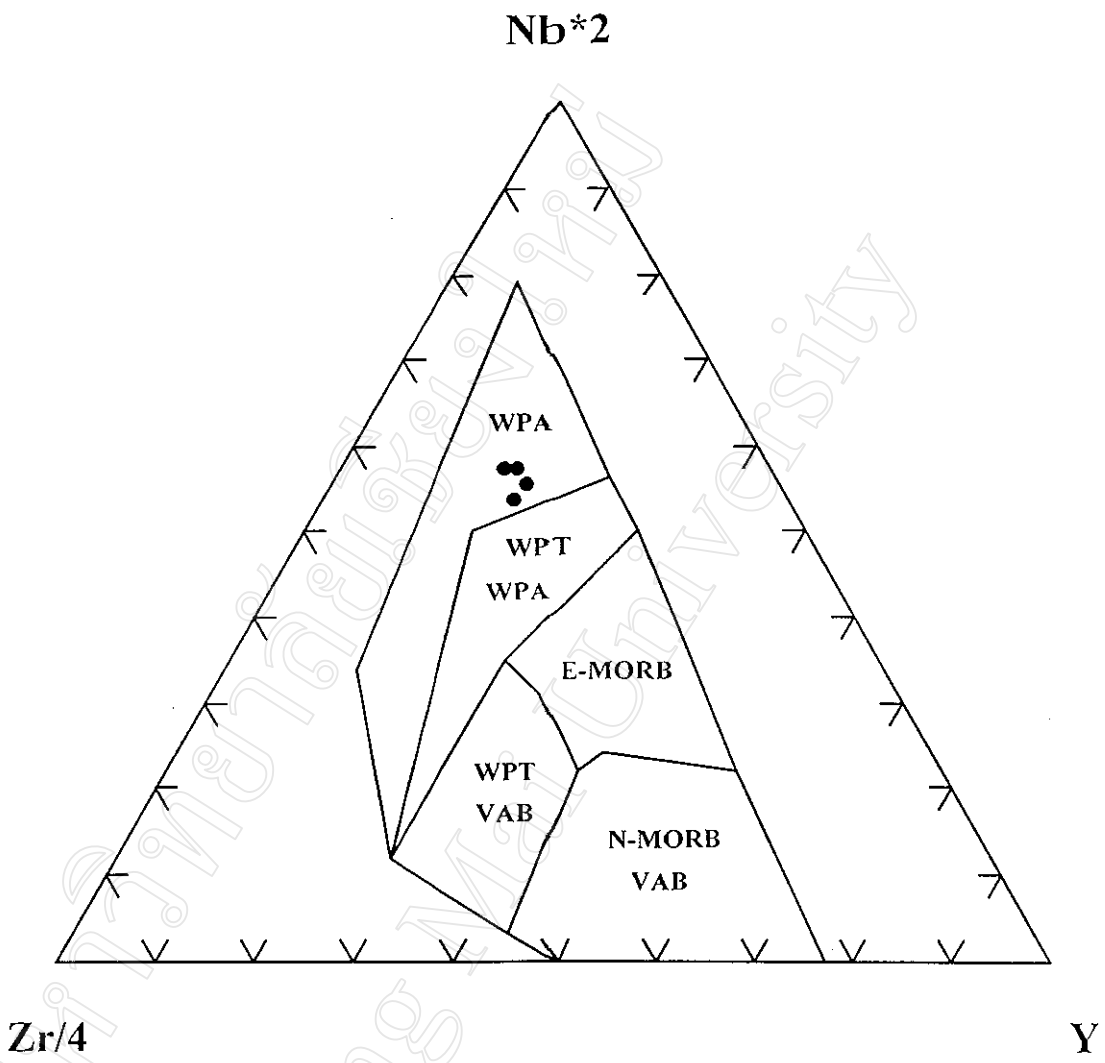

Figure 37 Nb-Zr-Y diagram for the analyzed Mae Tha basalts. Also shown are delimited fields for basalts of different tectonic environments (after Meschede, 1986). WPA = within-plate alkalic basalt, WPT = within-plate tholeiitic basalt, VAB = volcanic arc basalt, E-MORB = enriched mid-ocean ridge basalt, and N-MORB = normal mid-ocean ridge basalt.

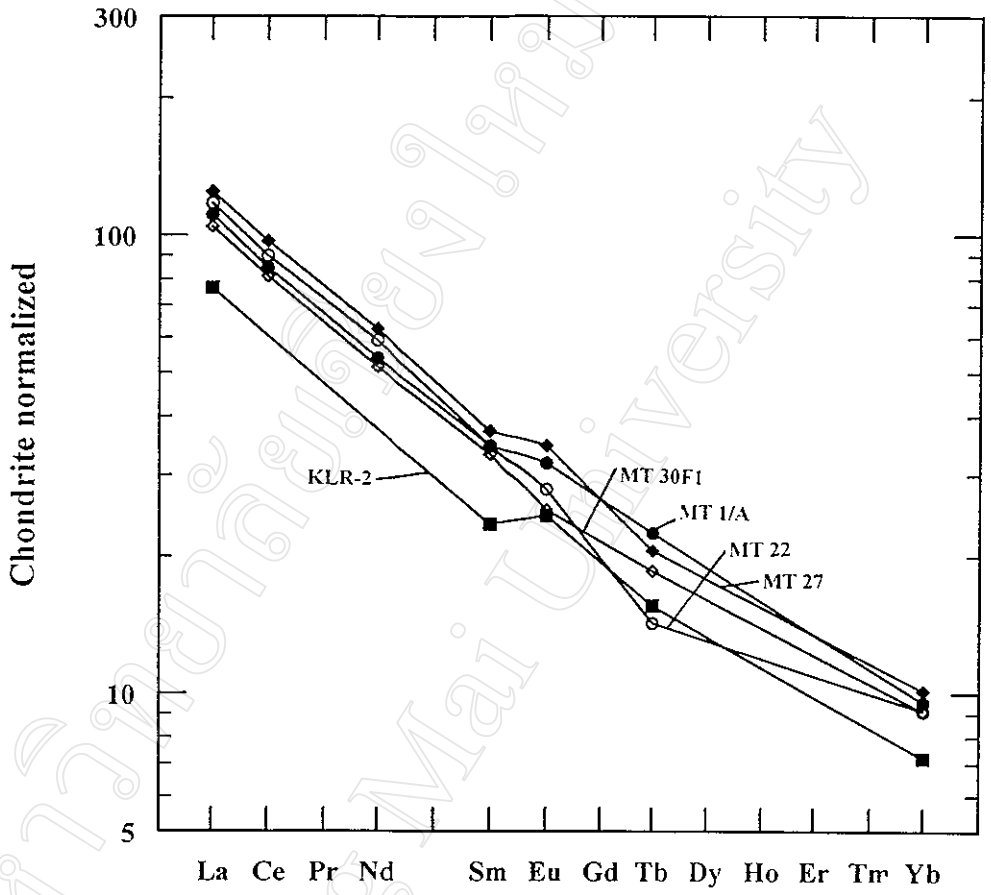

Figure 38 Chondrite-normalized REE patterns for the representative Mae Tha basalts (sample nos. MT 1/A, MT 22, MT 27 and MT 30F1) compared with that of the alkalic basalt from southern part of Gregory rift, Kenya (sample no. KLR-2). All the data of the modern analog are taken from Baker *et al.* (1977). Normalizing values used are those of Taylor and Gorton (1977).

So far, many sets of multi-element patterns have been proposed to characterize magmatic affinities. In this account, a N-MORB normalized multi-element plot of Pearce (1982, 1983) has been applied to the representatives of Mae Tha basaltic suite (Fig. 39). The N-MORB multi-element plot shows step-like patterns typical of within-plate alkalic basalts.

Many empirical diagrams for discriminating tectonic settings of eruption have appeared in literature (e.g. Figs. 36 and 37). Nevertheless, several subsequent studies, e.g. Holm (1982), Prestvik (1982), Duncan (1987) and Myers and Breitkopf (1989), have demonstrated that many empirical diagrams may often fail to clarify tectonic setting of eruption. Consequently, comparisons with modern lavas of different tectonic settings of formation have been carried out. The results, in terms of REE and N-MORB normalized multi-element patterns (Figs. 38 and 39), show that the Mae Tha basaltic lavas are closely analogous to the alkalic basalt from southern part of Gregory rift, Kenya (sample no. KLR-2), that have formed in the eastern branch of the Afro-Arabian rift system (Baker *et al.*, 1977). As a consequence, they are inferred to be alkalic basalts which erupted in a continental within-plate environment. This interpretation is consistent with the tectonic history of Thailand that the eruption of the Late Cenozoic basalts took place after the continent-continent collision between Shan-Thai and Indochina for a long period of time (e.g. Bunopas and Vella, 1983; Barr and MacDonald, 1991; Intasopa, 1993).

4.7 Chemical Stratigraphy

Since the Mae Tha basalts have undergone severe weathering and decomposition, it is impossible to correlate these flows at different locations, and envisage the total number of flows and stratigraphic sequence. Fortunately, there is a drill hole penetrating part of the basaltic pile in the vicinity of Ban Huai Rak Mai. Accordingly, chemical variation in successive liquids can be ascertained by plotting major and minor oxides, and trace elements of the flows penetrated in the drill hole against their elevations from a mean sea level (Figs. 40 and 41). Although these

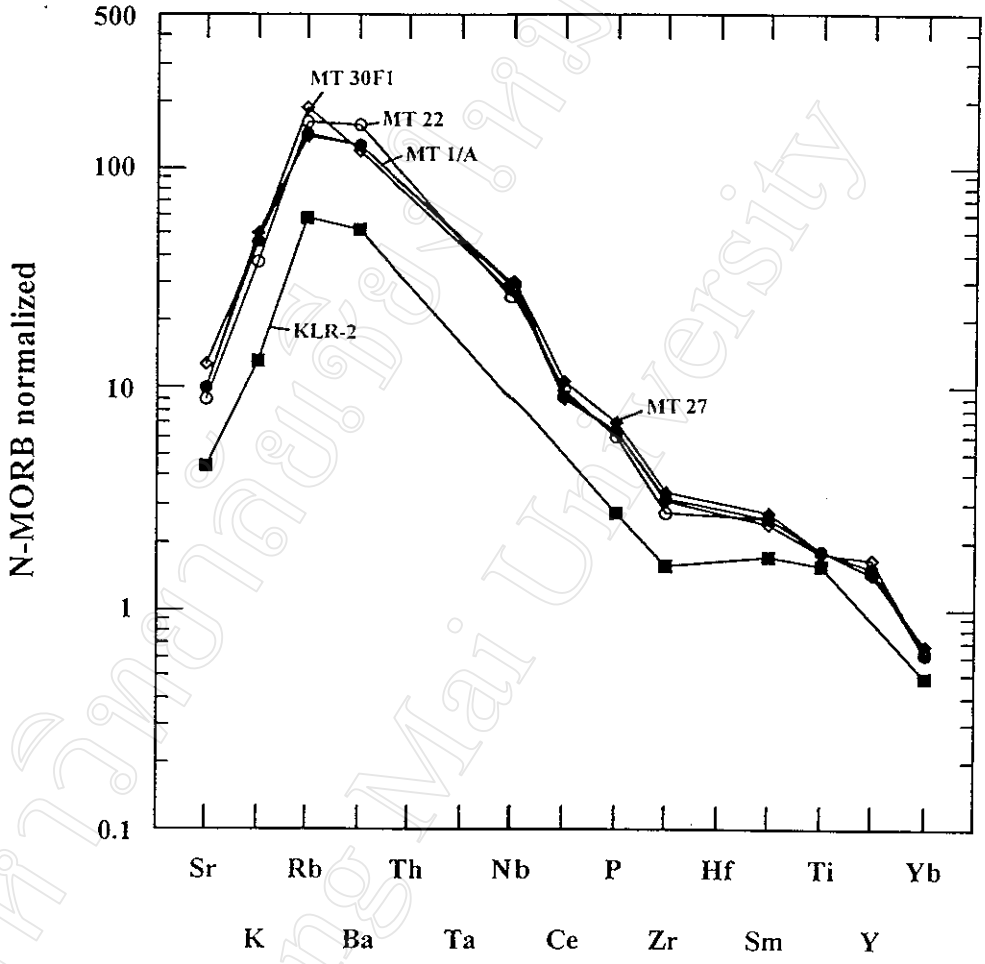

Figure 39 N-MORB normalized multi-element diagram of Pearce (1982, 1983) displaying the patterns for representative Mae Tha basalts (sample nos. MT 1/A, MT 22, MT 27 and MT 30F1) compared with that of the alkalic basalt from southern part of Gregory rift, Kenya (sample no. KLR-2). The source of data for the modern analog is the same as that in Figure 40. N-MORB normalizing values are those of Sun and McDonough (1989).

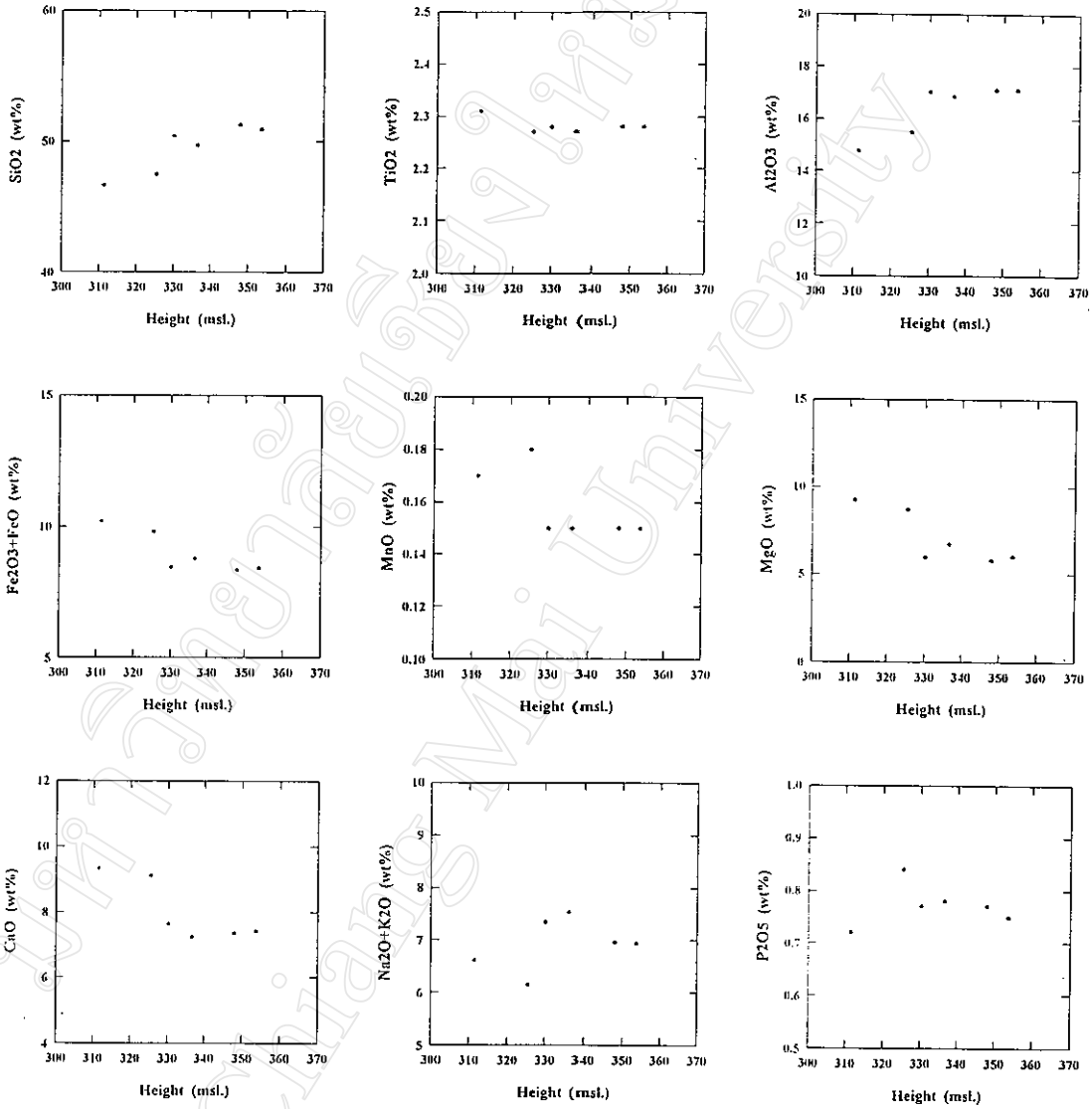

Figure 40 Major- and minor-oxide variation diagrams as a function of elevation above a mean sea level for the Mae Tha basalts penetrated in the drill hole at Ban Huai Rak Mai.

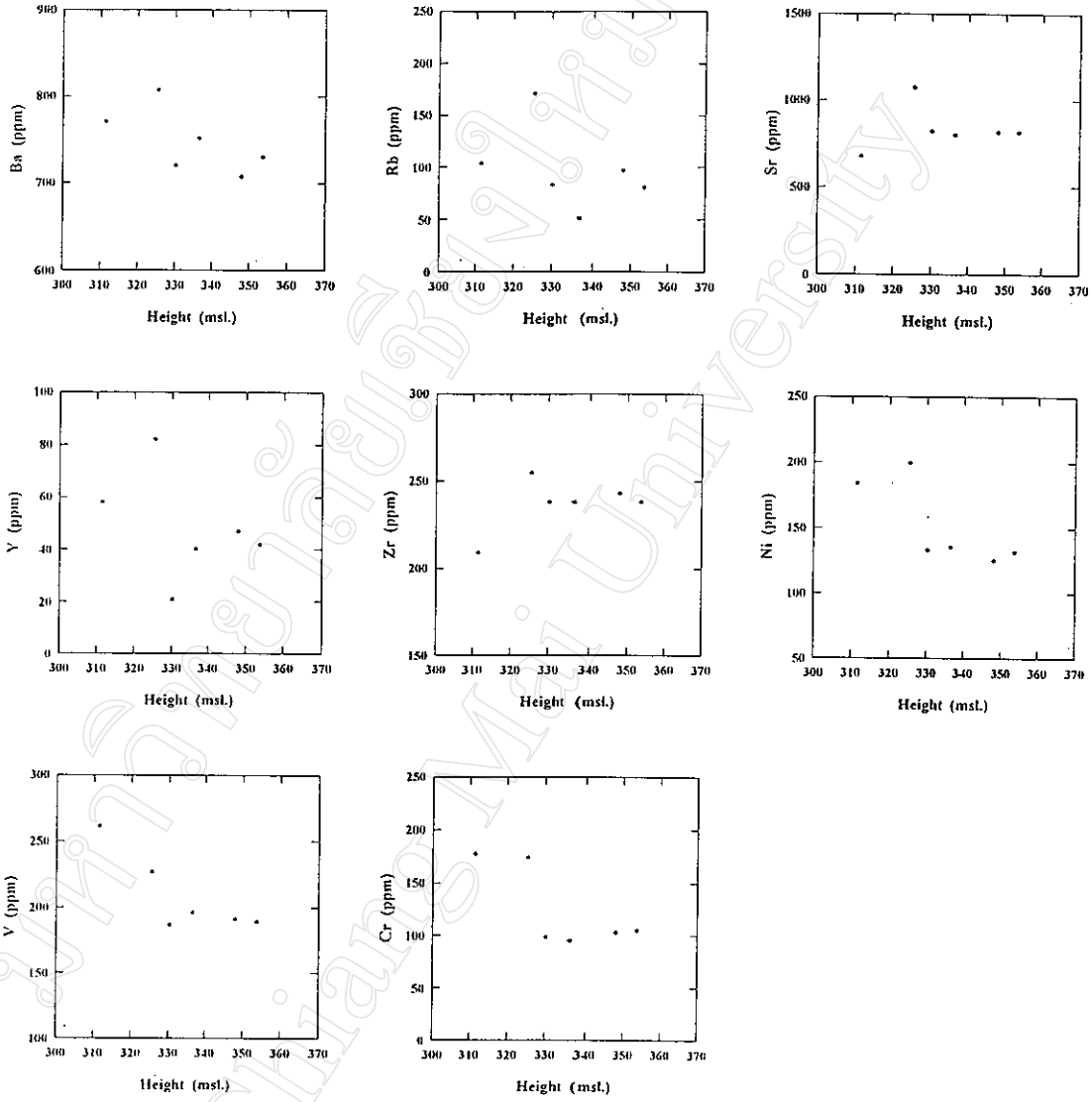

Figure 41 Trace-element variation diagrams as a function of elevation above a mean sea level for the Mae Tha basalts penetrated in the drill hole at Ban Huai Rak Mai.

elements show spike patterns with stratigraphy, they mainly form well-defined to broadly linear patterns. SiO_2, Al_2O_3 and $Na_2O + K_2O$ are enriched, whereas $FeO + Fe_2O_3$, MnO, MgO, CaO, V, Ni and Cr are depleted in the upper flows. These imply that the liquids giving rise to the Mae Tha basalts are generally more evolved with time. The depletion of Ba, Rb and Y in the upper flows, and the unclear P_2O_5, Sr and Zr patterns might be due to the limited values for fractionation parameter and analytical errors.